Published in Applied Energy with doi: 10.1016/j.apenergy.2023.121041

An Interval-based Privacy-Aware Optimization Framework for Electricity Price Setting in Isolated Microgrid Clusters

Marcos Tostado-Véliz[1], Hany M. Hasanien[2,3], Ahmad Rezaee Jordehi[4], Rania A. Turky[5], Manuel Gómez-González[1], Francisco Jurado[1,*]

1. Department of Electrical Engineering, University of Jaén, 23700 Linares, Spain (e-mail: mtostado@ujaen.es (M.T.-V.), mggonzal@ujaen.es (M.G.-G.) fjurado@ujaen.es (F.J.)).
2. Electrical Power and Machines Department, Faculty of Engineering, Ain Shams University, Cairo 11517, Egypt (e-mail: hanyhasanien@ieee.org).
3. Department of Electrical and Computer Engineering, Florida International University, Miami, FL 33174, USA.
4. Department of Electrical Engineering, Rasht Branch, Islamic Azad University, Rasht, Iran (e-mail: ahmadrezaeejordehi@gmail.com).
5. Electrical Engineering Department, Faculty of Engineering and Technology, Future University in Egypt, Cairo, Egypt (e-mail: Rania.turky@fue.edu.eg).

* Correspondence: fjurado@ujaen.es

Abstract. With the advance of communication infrastructures and the necessity of increasing the efficiency of energy systems, electricity networks are evolved towards more decentralized architectures and operational schemes. In this context, microgrid clusters are emerging as a valuable framework for optimal integrating renewable sources, demand response initiatives, and storage systems. When the cluster is competitive, the different agents partaking in the cluster compete for trading energy with others, for which an upstream agent (coordinator) sets nodal prices in a similar way to conventional energy markets. This paper is focused on this aspect by developing a novel price setting mechanism for islanded microgrid clusters based on an original equilibrium problem with an equilibrium constraints structure. The new proposal concerns about privacy issues, for which an original diagonalization algorithm is proposed by which only boundary information is transferred from microgrids to the coordinator. Moreover, uncertainties from renewable generation and demand are accommodated using interval notation and equivalent scenarios. The overall problem is raised as a bi-level model, which is further linearized and transformed into a single-level framework tractable by off-the-shelf solvers. A 4-microgrid cluster integrated into a 9-bus network serves as an illustrative case study. The impact of uncertainties is profusely studied, showing that total energy exchanged among microgrids can decrease by 61 % when the influence of uncertain parameters is notable. Other relevant aspects are discussed, and the practicability of the new proposal is demonstrated by analysing its computational performance. Moreover, the developed tool is further validated on a medium-scale network involving a large number of microgrids.

Keywords. Microgrid, Microgrid cluster, Peer-to-peer, Uncertainty

Nomenclature

Indices (Sets)	
i,j ($\mathbb{M}$)	Microgrid
t ($\mathbb{T}$)	Time
ω (Ω)	Scenario
m, n (Ψ)	Bus
$n \in \Psi_i$	i^{th} microgrid connected to the n^{th} bus
$m \in \Psi_n$	m^{th} bus connected to the n^{th} bus across a power line
ref	Reference bus

Superscripts	
$P2P, buy/sell$	Energy imported/exported from/to other microgrids
NS	Non-served
DG	Distributed generation
RES	Renewable generation
$BES, ch/dch$	Battery storage in charging/discharging mode
$\overline{(\cdot)}$	Maximum value of a variable or parameter
$(k)/(l)$	Outer/Inner loop iteration counter

Constants and parameters	
CI	Confidence interval [pu]
Δt	Time step [h]
C	Cost [$/pu·h]
a, b, c	Fuel cost of distributed generators [$/h, $/pu·h, $/pu²·h]
RD/RU	Downward/Upward ramping rate [pu]
η	Efficiency [pu]
$\mathbf{B}$	Susceptance matrix of the network [pu]
M	Large positive number ~10^5 [-]
$\epsilon^{MG}/\epsilon^{EPEC}$	Outer/Inner loop convergence threshold [-]

Decision variables	
p	Power [pu]
y	Commitment status [Binary]
ε	Energy [pu·h]
α	Bid/Offer price [$/pu·h]
θ	Nodal angle [rad]
ξ	Auxiliary variable for linearization of complementarity terms [Binary]

Decision variables (dual problem)	
$\underline{\mu}^{P2P,buy}/\underline{\mu}^{P2P,sell}$	Dual variable from minimum importable/exportable power [-]
$\overline{\mu}^{P2P,buy}/\overline{\mu}^{P2P,sell}$	Dual variable from maximum importable/exportable power [-]
$\underline{\zeta}/\overline{\zeta}$	Dual variable from maximum power flow through lines [-]
$\underline{\gamma}/\overline{\gamma}$	Dual variable from minimum/maximum nodal angle [-]
$\gamma_{\omega,ref,t}$	Dual variable from reference angle [-]
λ	Nodal price [$/pu·h]

1 - Introduction

1.1 - Context and motivation

With the advance of communication infrastructures and the necessity of decarbonizing the electricity sector, distribution systems are evolved towards active architectures in which consumers actively partake in the operation of the network [1]. In such context, microgrids (MGs) appear as an invaluable framework for optimal integrating renewable energy sources (RESs), storage systems, and demand response (DR) at low-, and medium-voltage scales [2]. A group of MGs can interact among themselves when located in the same geographical area and interconnected across power lines. This emerging paradigm is known as MG cluster (MGC) and calls up for new operational and economic models that enable the optimal coordination of the different agents involved [3]. In such systems, new concepts such as peer-to-peer (P2P) energy trading are gaining importance [4], thus enabling energy transactions among MGs improving the efficiency of the cluster.

Motivated by the more active interactions among MGs, new operational tools are necessary which allow fair and effective trading mechanisms. In this regard, the figure of the MGC coordinator becomes necessary to establish the trading mechanisms and set energy prices in the cluster. This upcoming agent requires the use of new computational tools that, unlike existing methods, consider the preferences of peers within a competitive environment besides privacy concerns. This paper is focused on the role of the MGC coordinator and her importance in encouraging users to partake in P2P energy trading within the cluster. To this end, a new price setting mechanism with privacy consideration under uncertainty is developed.

1.2 - Related works

The concept of MGC is relatively new and became to be seriously studied in the mid-2010s [5]. Nevertheless, the importance of optimally coordinating groups of MGs was previously identified, although those original works normally recurred to the term 'multi-microgrid', which refers to a group of MGs that interact in different ways without necessarily exchanging energy under a fair and effective market mechanism. Jalali et al. [6] developed a decision-making framework for distribution system operations in the presence of MGs. This reference proposes a game-based bi-level optimization scheme to model the interactions among the network and the MGs connected to it, focusing on the role of DR initiatives. In [7], a two-level clearing mechanism was developed in which the distribution network operator acts as the leader, operating the grid and calculating the trading prices, while interconnected MGs act as followers in a Stackelberg-based paradigm. A two-stage mechanism for coordinating distribution networks and MGs was established in [8], considering uncertainties in renewable generation and loads using robust sets and the column-and-constraint generation algorithm is used for converting the original nonlinear problem into a mixed-integer-linear programming (MILP). In [9], a four-layer mechanism was developed, for local P2P trading in MGs. Then, energy transactions among agents are performed on the basis of heuristic mechanisms, showing that P2P may help to improve the local balance in the grid.

In [10], a mathematical programming with equilibrium constraints (MPEC) stochastic model was introduced for optimal coordination of distribution network and MGs. In this model, the distribution network operator deals with decisions in day-ahead and real-time scenarios, modelling the uncertainties through stochastic modelling. Zhou and Ai [11], introduced the concept of combined cooling-heating MGCs, and developed a clearing strategy for such frameworks based on different consensus and distributed algorithms. In [12], a hierarchical bi-level optimization framework was developed for optimal coordination of MGs, considering the figure of an aggregator, who concerns about interactions among agents in a cooperative way. A day-ahead scheduling mechanism for cooperative energy communities was proposed in [13]. The new proposal accounts for privacy concerns by exchanging limited information within a distributed framework, for which a methodology based on alternating direction of multipliers was developed. Zhou, et al. [14] developed two different algorithms for solving the coordination problem among MGs and the distribution network operator. In this regard, column-and-constraint generation and target cascading algorithms are applied in a decentralized manner, incorporating uncertainties via robust modelling. Likewise, a decentralized algorithm based on alternating direction of multipliers was applied in [15] for islanded multi-MGs systems. Rodrigues, et al. [16] proposed a battery sizing methodology for P2P trading platforms. The new methodology was a manageable MILP and was applied to a campus building exhibiting good results. In [17], a MPEC model was developed for optimal coordination in non-cooperative MGCs connected through AC/DC networks, incorporating uncertainties using robust optimization solved by column-and-constraint generation algorithm. Naebi, et al. [18] proposed an equilibrium problem with equilibrium constraints (EPEC) framework, for optimal bidding strategy of multi-MGs in distribution networks.

In [19], a hierarchical framework was developed for optimal coordination of DC MGCs, considering optimal response of controllers against power fluctuations through droop curves. The overall optimization problem is then solved in a distributed manner under uncertainties. Nezamabadi and Vahidinasab [20] proposed an optimal bidding strategy for strategic MGs in competitive P2P environments based on a MPEC optimization model, considering risk-averse strategies through enforcing the conditional value-at-risk. In [21], a decentralized model for electric-heat-cool MGCs was developed. The optimization problem is based on the different owners of each MG within the cluster, for which a decentralized solution methodology based on alternating direction of multipliers is employed. A bi-level solution methodology for optimal P2P trading among MGs connected to distribution networks was developed in [22]. This reference proposed two distributed algorithms for optimal power allocation throughout the network based on the theoretical optimal behavior of buyers and sellers. Sheikhahmadi, et al. [23] established an

EPEC mechanism for optimal participation of multi-MGs systems in local energy and reserve markets considering the presence of interruptible loads. A risk trading mechanism for communities was developed in [24]. In this reference, via chance-constrained formulation, the different prosumers in a community can manage the conservativeness assumed in day-ahead decisions via financial products. In [25], a coordinated framework for day-ahead and intra-day decision-making in local energy communities was developed. As in [13], the new methodology accounts for limited information exchanging within a distributed algorithm whereas uncertainties in intra-day decisions are managed via scenarios.

Table 1 - A summary of the literature review

Refs.	**System**	**Model**	**Uncertainties**	**Privacy**
[6, 12]	Multi-MGs	Bi-level	No	No
[7, 8, 14]	Multi-MGs	Bi-level	Robust	No
[9]	MG	Single-level	No	No
[10]	Multi-MGs	Bi-level	Stochastic	No
[11]	MGC	Consensus	Chance-constrained	No
[13]	Community	Single-level	No	Yes
[15]	Multi-MGs	Bi-level	No	Yes
[16]	MG	Single-level	No	No
[17]	MGC	Bi-level	Robust	No
[18, 23]	Multi-MGs	EPEC	No	No
[19]	MGC	Bi-level	Robust	Yes
[20]	Multi-MGs	Bi-level	Interval	No
[21]	MGC	Decentralized	Stochastic	Yes
[22]	Multi-MGs	Decentralized	No	Yes
[24]	Community	Single-level	Stochastic	Yes
[25]	Community	Single-level	Chance-constrained	No
Present	MGC	EPEC	Interval	Yes

1.3 - Research gaps and contributions

This paper addresses the issue of optimal pricing in islanded MGCs under uncertainties. To this end, an EPEC approach is raised, which solves the bi-level problem associated to each participant sequentially using diagonalization. As result, the equilibrium nodal prices are obtained together with the optimal bidding strategy of each MG partaking in the cluster. The overall problem is formulated as a MILP, for which each bi-level individual problem is transformed into a single-level one using its Karush-Kuhn-Tucker (KKT) conditions and further linearized through different tricks. Uncertainties from RESs and inelastic demand are modelled using interval notation and equivalent scenarios [20]. One of the main advantages of the present work with respect others is the limited amount of information that must be transferred from MGs to the upper level managed by a coordinator. In contrast to other works that recur to iterative algorithms and nonlinear formulations, privacy of users is ensured in this work by only exchanging boundary information with the cluster coordinator, which is very suitable for competitive platforms where interests of individuals may be conflictive.

In the rest of this paper, Section 2 overviews the proposed MGC structure and its price setting mechanism, and introduce the uncertainties modelling used in this paper. Section 3 describes the operational model of each MG, which is essential for the developed setting process, which is formally introduced in Section 4 from the original bi-level nonlinear problem to the resulting single-level MILP. Section 5 describes the privacy-aware diagonalization-based solution algorithm. Section 6 presents a case study with results. Lastly, Section 7 concludes the paper.

2 - Preliminaries

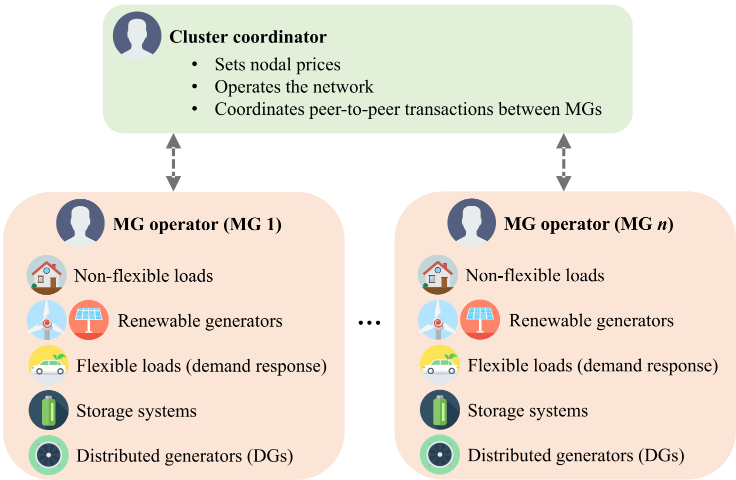

Fig. 1 - Sketch of the proposed cluster structure

2.1 - The proposed cluster framework

For solving the pricing problem in islanded MGCs, we propose a two-level structure as depicted in Fig. 1. Let us assume that n MGs with different owners are connected to the same network (typically at medium-voltage level). Furthermore, each MG encompasses on-site renewable and distributed generators (DGs), storage systems and local demand (flexible and non-flexible), which are managed by the different MG operators. Daily, each MG can partake in local energy trading under nodal prices. This task is performed by the cluster coordinator, who also ensures safe and reliable supplying to all the users connected to the network. This agent daily performs the price setting process and schedules the energy transactions among peers, ensuring that the market result is technically feasible and maximizes the collective welfare. In the proposed structure, MGs are assumed to be reluctant to share information with other agents. In this regard, we assume that only boundary information (maximum exchangeable energy and bidding/offering price) can be shared with the coordinator, while the rival MGs cannot receive information from other peers. Note that this information is the minimum necessary to perform a fair market mechanism and usually shared in energy markets [26].

2.2 - Uncertainties modelling

In the price setting process described above there are two main sources of uncertainties. On the one hand, renewable generation is uncertain in nature as it strongly depends on weather parameters (wind speed, temperature and solar irradiance). On the other hand, non-flexible demand depends on human decisions which are actually random. Although these two uncertainties can be forecasted with acceptable accurateness, their actual realization can deviate from predicted values and impact notably in the final result. In this regard, we assume that MG operators and cluster coordinator are keen on obtaining an uncertainty-aware result that takes into account possible deviations from predicted values.

To cope with uncertainties, there exists multiple approaches in the literature. Broadly, uncertainty models are classified into probabilistic and robust [27]. Probabilistic approaches (also called stochastic) are based on generating a large number of scenarios for possible uncertainties realization. Then, the most probable result is calculated. In this sense, probabilistic approaches are not, in general, able to reproduce risk-averse or risk-seeker results. On contrary, robust models seek for the worst/best realization of uncertainties. Among the most popular robust approaches, one can find the information gap decision theory and interval notations [28, 29]. These approaches, although quite useful, may complicate the formulation of the problem leading to nonlinear models unsolvable by off-the-shelf solvers. In order to overcome the issues of each methodology, we propose to use an interval-based model derived from stochastic approaches [20], which is explained below.

Let us represent the uncertain parameter φ as an interval number by its expected value $\mathrm{E}(\varphi)$ and the corresponding confidence interval $CI \in \mathbb{R}_{+}$, as follows [28].

$$\varphi \in [\mathrm{E}(\varphi) - CI \cdot \mathrm{E}(\varphi), \mathrm{E}(\varphi) + CI \cdot \mathrm{E}(\varphi)] \tag{1}$$

The notation above is sketched in Fig. 2 and has been successfully applied in different optimization problems under uncertainty [28, 30]. However, the interval notation (1) cannot be easily accommodated in MILP problems (bi-level frameworks and iterative algorithms have been proposed in the literature [30, 31]). To easily manage the model (1) and preserve the linear feature of the mathematical formulation, we transform the interval number (1) into three equi-probable scenarios, as follows [20].

$$\varphi = \begin{cases} \mathrm{E}(\varphi) - CI \cdot \mathrm{E}(\varphi) \\ \mathrm{E}(\varphi) \\ \mathrm{E}(\varphi) + CI \cdot \mathrm{E}(\varphi) \end{cases} \tag{2}$$

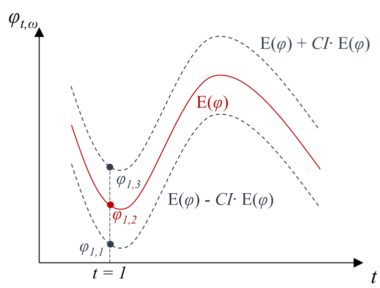

Fig. 2 - Illustration of the interval modelling and its transformation in equivalent scenarios

Indeed, each uncertainty is thus defined by its expected value together with its minimum and maximum bounds given by the confidence interval. When different uncertainties are involved, the resulting scenarios must be coherent. It means that equivalent scenarios of different uncertainties respond to the worst or best realization of each parameter, regardless each scenario is given for the upper and lower bound of each parameter. To better illustrate this point, let us consider the two sources of uncertainties involved in our problem, i.e. renewable generation and non-flexible demand. To use the uncertainty model (2), one should relate the bounds of each uncertainty so that the worst/best realization of uncertainties is captured. For our cluster, DGs have an associated fuel cost while renewable generation is assumed to be free. Therefore, assuming the total cost of the cluster as the objective function, it is clear that the most pessimistic conditions would be given when the highest demand coincides with the lowest renewable generation. Under these conditions, distributed generators will be called more frequently to satisfy the demand, which is scarcely satisfied through renewable generators because their low expected potential. This intuitive interpretation can be easily adopted for deducing the most optimistic conditions, which would be given when the non-flexible demand is minimum and the renewable generation is maximum. Note that these similar conclusions were already drawn in [20] and allow to discard other intermediate scenarios, which will always yield a total cost between the two bounds calculated by the methodology explained above. This way, a risk-averse/seeker result can be obtained without needing of recurring to interval or other more complex notations. This evidence is empirically demonstrated in Section 6.

3 - MG operational model

As described in Section 5, the developed price setting mechanism needs to previously define each MG as buyer or seller each time period. To this end, the day-ahead optimal energy management of each MG (3)-(18) needs to be solved assuming known nodal prices.

$$\max_{\mathbf{x}_i^{MG}} \sum_{\omega\in\Omega} \left\{ \frac{\Delta t}{|\Omega|} \cdot \sum_{t\in\mathbb{T}} \left\{ \begin{matrix} \alpha_{i,t} \cdot \left(p_{i,\omega,t}^{P2P,sell} - p_{i,\omega,t}^{P2P,buy}\right) - C_i^{NS} \cdot p_{i,\omega,t}^{NS} \\ -C_{i,\omega,t}^{DG} - C_i^{DR} \cdot \left(\overline{p}_{i,\omega,t}^{DR} - p_{i,\omega,t}^{DR}\right) \end{matrix} \right\} \right\} \tag{3}$$

Subject to:

$$C_{i,\omega,t}^{DG} = y_{i,t}^{DG} \cdot a_i^{DG} + p_{i,\omega,t}^{DG} \cdot b_i^{DG} + \left(p_{i,\omega,t}^{DG}\right)^2 \cdot c_i^{DG}; \forall\omega \in \Omega \wedge t \in \mathbb{T} \tag{4}$$

$$\left\{ \begin{matrix} p_{i,\omega,t}^{P2P,buy} + p_{i,\omega,t}^{DG} + p_{i,\omega,t}^{RES} + p_{i,\omega,t}^{BES,dch} + \\ p_{i,\omega,t}^{NS} = p_{i,\omega,t}^{P2P,sell} + p_{i,\omega,t}^{NC} + p_{i,\omega,t}^{DR} + p_{i,\omega,t}^{BES,ch} \end{matrix} \right. ; \forall\omega \in \Omega \wedge t \in \mathbb{T} \tag{5}$$

$$p_{i,\omega,t}^{NS} \geq 0; \forall\omega \in \Omega \wedge t \in \mathbb{T} \tag{6}$$

$$y_{i,t}^{DG} \cdot \underline{p}_i^{DG} \leq p_{i,\omega,t}^{DG} \leq y_t^{DG} \cdot \overline{p}_i^{DG}; \forall\omega \in \Omega \wedge t \in \mathbb{T} \tag{7}$$

$$RD_i^{DG} \leq p_{i,\omega,t}^{DG} - p_{\omega,t-1}^{DG} \leq RU_i^{DG}; \forall\omega \in \Omega \wedge t \in \mathbb{T}\backslash t = 1 \tag{8}$$

$$p_{i,\omega,t}^{RES} \leq \overline{p}_{i,\omega,t}^{RES}; \forall\omega \in \Omega \wedge t \in \mathbb{T} \tag{9}$$

$$p_{i,\omega,t}^{BES,x} \leq \overline{p}_i^{BES}; \forall\omega \in \Omega \wedge t \in \mathbb{T} \wedge x \in \{ch, dch\} \tag{10}$$

$$\varepsilon_{i,\omega,t}^{BES} = \varepsilon_{i,\omega,t-1}^{BES} + \Delta t \cdot \left(\eta_i^{BES} \cdot p_{i,\omega,t}^{BES,ch} - \frac{p_{i,\omega,t}^{BES,dch}}{\eta_i^{BES}}\right); \forall\omega \in \Omega \wedge t \in \mathbb{T}\backslash t = 1 \tag{11}$$

$$\underline{\varepsilon}_i^{BES} \leq \varepsilon_{i,\omega,t}^{BES} \leq \overline{\varepsilon}_i^{BES}; \forall\omega \in \Omega \wedge t \in \mathbb{T} \tag{12}$$

$$\varepsilon^{BES}_{i,\omega,\mathbb{T}[1]} = \varepsilon^{BES}_{i,\omega,|\mathbb{T}|} = \overline{\varepsilon}^{BES}_{i}; \forall \omega \in \Omega \tag{13}$$

$$\underline{p}^{DR}_{i,\omega,t} \leq p^{DR}_{i,\omega,t} \leq \overline{p}^{DR}_{i,\omega,t}; \forall \omega \in \Omega \wedge t \in \mathbb{T} \tag{14}$$

$$p^{P2P,x}_{i,\omega,t} \leq \overline{p}^{P2P}; \forall \omega \in \Omega \wedge t \in \mathbb{T} \wedge x \in \{buy, sell\} \tag{15}$$

$$0 \leq p^{BES,ch}_{i,\omega,t} \perp p^{BES,dch}_{i,\omega,t} \geq 0; \forall \omega \in \Omega \wedge t \in \mathbb{T} \tag{16}$$

$$0 \leq p^{P2P,buy}_{i,\omega,t} \perp p^{P2P,sell}_{i,\omega,t} \geq 0; \forall \omega \in \Omega \wedge t \in \mathbb{T} \tag{17}$$

$$y^{DG}_{i,t} \in \{0,1\}; \forall t \in \mathbb{T} \tag{18}$$

where $\mathbf{X}^{MG}_{i}$ is the vector of decision variables for the i^{th} MG within the cluster and $\perp$ denotes orthogonality. Note that the problem above must be solved $\forall i \in \mathbb{M}$.

The objective function of the MG operational model seeks to maximize the monetary revenue by trading energy in local markets, discounting the non-served, DR and fuel expenditures of DGs, which are defined as a quadratic function in (4) [31]. On the other hand, (5) is the MG power balance while (6) ensures that the non-served power is positive. The power and ramp limits of DGs are represented in (7) and (8), respectively. The maximum generation of RESs is limited by (9) whereas (10) upper bounds the power exchanged by storage systems to rated values. The state-of-charge of storage systems is modelled with (11) being limited by (12), while (13) fixes the total initial and final energy stored. The DR initiatives are modelled by (14), considering curtailment programs, while (15) limits the power that can be traded with the cluster through P2P exchanges. Lastly, (16) imposes complementarity in the charging and discharging processes of batteries, (17) avoids that the i^{th} MG can simultaneously partake as a buyer and a seller, and (18) imposes integrity in the commitment statuses of DGs.

As mentioned, the model (3)-(18) assumes that nodal prices are known, which is unrealistic since the MGs in the cluster are price-takers and nodal prices are fixed by the coordinator after the price setting process. In the developed solution methodology, this is solved by iteratively updating the nodal prices (see Section 5). It is also worth noting that the continuous variables in (3)-(18) are defined over the dimension ω, which has size three for accommodating the equivalent scenarios derived from the interval notation described in Section 2. This way, uncertainties from renewable generation and inelastic demand are handled.

4 - Nodal price model

4.1 - Upper level: optimal bidding/offering strategy

The price setting model is raised as a bi-level optimization framework, as usually [32], whose structure is depicted in Fig. 3. In the upper level, the optimal bidding/offering strategy of the i^{th} MG partaking in the cluster is defined after solving the following optimization problem.

$$\max_{\mathbf{X}^{UL}_{i} \cup \alpha_{i,t}} \sum_{\omega \in \Omega} \left\{ \frac{\Delta t}{|\Omega|} \cdot \sum_{t \in \mathbb{T}} \left\{ \lambda_{n \in \Psi_{i},\omega,t} \cdot \left(p^{P2P,sell}_{i,\omega,t} - p^{P2P,buy}_{i,\omega,t} \right) \right\} \right\} \tag{19}$$

Subject to

$$\alpha_{i,t} \geq 0; \forall t \in \mathbb{T} \tag{20}$$

where $\mathbf{X}_i^{UL}$ is the vector of decision variables of the upper level of the i^{th} MG. As seen, the problem above seeks the optimal market strategy for maximizing the revenue of the MG, for which the offering/bidding price is taking as a variable.

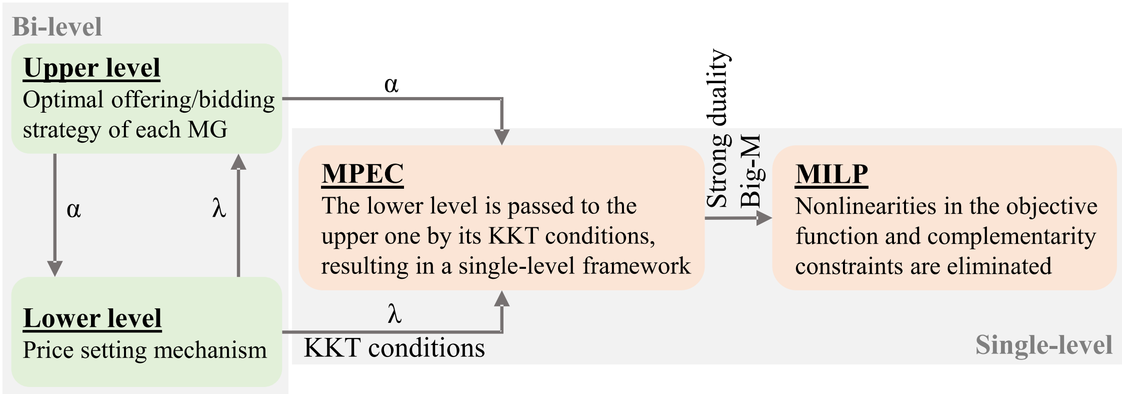

Fig. 3 - Structure of the proposed bi-level model and the resulting single-level problem

4.2 - Lower level: price setting

In the lower level, the cluster coordinator sets nodal prices taking the network into consideration, for which the following optimization model is solved.

$$\max_{\mathbf{X}_{primal}^{LL}} \sum_{\omega\in\Omega}\sum_{i\in\mathbb{M}}\sum_{t\in\mathbb{T}}\left\{\alpha_{i,t}\cdot\left(p_{i,\omega,t}^{P2P,buy}-p_{i,\omega,t}^{P2P,sell}\right)\right\} \tag{21}$$

Subject to:

$$\begin{cases}\sum_{m\in\Psi_n}\mathbf{B}_{[n,m]}\cdot\left(\theta_{\omega,n,t}-\theta_{\omega,m,t}\right)\\+\sum_{i\in\Psi_n}\left(p_{i,\omega,t}^{P2P,buy}-p_{i,\omega,t}^{P2P,sell}\right)=0\end{cases}:\lambda_{n,\omega,t};\forall\omega\in\Omega\wedge n\in\Psi\wedge t\in\mathbb{T} \tag{22}$$

$$p_{i,\omega,t}^{P2P,buy}\le\overline{p}_{i,\omega,t}^{P2P,buy}:\underline{\mu}_{i,\omega,t}^{P2P,buy},\overline{\mu}_{i,\omega,t}^{P2P,buy};\forall i\in\mathbb{M}\wedge\omega\in\Omega\wedge t\in\mathbb{T} \tag{23}$$

$$p_{i,\omega,t}^{P2P,sell}\le\overline{p}_{i,\omega,t}^{P2P,sell}:\underline{\mu}_{i,\omega,t}^{P2P,sell},\overline{\mu}_{i,\omega,t}^{P2P,sell};\forall i\in\mathbb{M}\wedge\omega\in\Omega\wedge t\in\mathbb{T} \tag{24}$$

$$-\overline{F}_{[n,m]}\le F_{\omega,[n,m],t}\le\overline{F}_{[n,m]}:\underline{\zeta}_{\omega,[n,m],t},\overline{\zeta}_{\omega,[n,m],t};\forall i\in\mathbb{M}\wedge\omega\in\Omega\wedge m,n\in\Psi\wedge t\in\mathbb{T} \tag{25}$$

$$F_{\omega,[n,m],t}=\mathbf{B}_{[n,m]}\cdot\left(\theta_{\omega,n,t}-\theta_{\omega,m,t}\right);\forall\omega\in\Omega\wedge n,m\in\Psi\wedge t\in\mathbb{T} \tag{26}$$

$$-\pi\le\theta_{\omega,n,t}\le\pi:\underline{\gamma}_{\omega,n,t},\overline{\gamma}_{\omega,n,t};\forall\omega\in\Omega\wedge n\in\Psi\backslash n=ref\wedge t\in\mathbb{T} \tag{27}$$

$$\theta_{\omega,ref,t}=0:\gamma_{\omega,ref,t};\forall\omega\in\Omega\wedge t\in\mathbb{T} \tag{28}$$

where $\mathbf{X}_{primal}^{LL}$ collects the primal variables of the lower level. The lower level seeks to maximize the collective welfare given in (21) while ensures the reliability of the network. Thus, (22) represents the nodal balance, (23) and (24) limits the power that can be traded by MGs, (25) limits the power flow across branches as calculated by (26), while (27) imposes limits in the nodal angles, being fixed at the reference bus by (28). Note that in constraints (22)-(28), the corresponding dual variables are given at the right-hand side of each equation.

4.3 - MPEC

The bi-level problem presented in Section 4.1 and Section 4.2 cannot be solved directly. Instead, the lower level problem is transferred to the upper level by its KKT conditions as shown in Fig. 3, resulting in the following single-level MPEC framework.

Maximize: (19)

Subject to (20), (22)-(28) and

$$-\alpha_{i,t}-\underline{\mu}_{i,\omega,t}^{P2P,buy}+\overline{\mu}_{i,\omega,t}^{P2P,buy}+\lambda_{n\in\Psi_i,\omega,t}=0;\forall i\in\mathbb{M}\wedge\omega\in\Omega\wedge t\in\mathbb{T} \quad (29)$$

$$\alpha_{i,t}-\underline{\mu}_{i,\omega,t}^{P2P,sell}+\overline{\mu}_{i,\omega,t}^{P2P,sell}-\lambda_{n\in\Psi_i,\omega,t}=0;\forall i\in\mathbb{M}\wedge\omega\in\Omega\wedge t\in\mathbb{T} \quad (30)$$

$$\sum_{m\in\Psi_n}\left\{\begin{matrix}\mathbf{B}_{[n,m]}\cdot\Big(\lambda_{n,\omega,t}-\lambda_{m,\omega,t}+\overline{\zeta}_{\omega,[n,m],t}\\-\underline{\zeta}_{\omega,[m,n],t}-\underline{\zeta}_{\omega,[n,m],t}+\underline{\zeta}_{\omega,[m,n],t}\Big)\end{matrix}\right\}-\underline{\gamma}_{\omega,n,t}+\overline{\gamma}_{\omega,n,t}=0;\forall\omega\in\Omega\wedge n\in\Psi\backslash n=ref\wedge t\in\mathbb{T} \quad (31)$$

$$\sum_{m\in\Psi_{ref}}\left\{\begin{matrix}\mathbf{B}_{[ref,m]}\cdot\Big(\lambda_{ref,\omega,t}-\lambda_{m,\omega,t}+\overline{\zeta}_{\omega,[ref,m],t}\\-\underline{\zeta}_{\omega,[m,ref],t}-\underline{\zeta}_{\omega,[ref,m],t}+\underline{\zeta}_{\omega,[m,ref],t}\Big)\end{matrix}\right\}+\gamma_{\omega,ref,t}=0;\forall\omega\in\Omega\wedge t\in\mathbb{T} \quad (32)$$

$$0\leq\begin{matrix}\overline{\mu}_{i,\omega,t}^{P2P,x}\perp\left(\overline{p}_{i,\omega,t}^{P2P,x}-p_{i,\omega,t}^{P2P,x}\right)\\\underline{\mu}_{i,\omega,t}^{P2P,x}\perp p_{i,\omega,t}^{P2P,x}\end{matrix}\geq 0;\forall i\in\mathbb{M}\wedge\omega\in\Omega\wedge t\in\mathbb{T}\wedge x\in\{buy,sell\} \quad (33)$$

$$0\leq\begin{matrix}\underline{\zeta}_{\omega,[n,m],t}\perp\left(F_{\omega,[n,m],t}+\overline{F}_{[n,m]}\right)\\\overline{\zeta}_{\omega,[n,m],t}\perp\left(\overline{F}_{[n,m]}-F_{\omega,[n,m],t}\right)\end{matrix}\geq 0;\forall\omega\in\Omega\wedge m,n\in\Psi\wedge t\in\mathbb{T} \quad (34)$$

$$0\leq\begin{matrix}\underline{\gamma}_{\omega,n,t}\perp\left(\theta_{\omega,n,t}+\pi\right)\\\overline{\gamma}_{\omega,n,t}\perp\left(\pi-\theta_{\omega,n,t}\right)\end{matrix}\geq 0;\forall\omega\in\Omega\wedge n\in\Psi\backslash n=ref\wedge t\in\mathbb{T} \quad (35)$$

$$\left\{\begin{matrix}\underline{\mu}_{i,\omega,t}^{P2P,x},\overline{\mu}_{i,\omega,t}^{P2P,x},\\\underline{\zeta}_{\omega,[n,m],t},\overline{\zeta}_{\omega,[n,m],t},\\\underline{\gamma}_{\omega,n,t},\overline{\gamma}_{\omega,n,t},\gamma_{\omega,ref,t}\end{matrix}\right.\geq 0;\forall i\in\mathbb{M}\wedge\omega\in\Omega\wedge m,n\in\Psi\wedge t\in\mathbb{T}\wedge x\in\{buy,sell\} \quad (36)$$

The feasibility of the original lower level is ensured by including in the constraints (22)-(28). On the other hand, (29)-(32) are the stationary conditions derived from the Lagrangian function of (19) (see Appendix A), while (33)-(35) are the complementarity constraints of the dual problem. Lastly, (36) imposes positiveness in dual variables.

Note that in other similar works (e.g. see [17]), the upper level is extended by incorporating the model (3)-(18) and those constraints are included in the MPEC to ensure its feasibility. However, in the proposed cluster, the MPEC above is performed by the coordinator while each MG operator runs her own operational model as described in Section 3. This way, if the constraints (3)-(18) are included in the MPEC, privacy of MG owners is no longer preserved as the coordinator needs to access to confidential information (e.g. data of flexible demands or DGs). This is the reason why we did not include the model (3)-(18) in the MPEC problem above, while its feasibility is ensured yet by iteratively updating the upper bounds in (23) and (24), as explained in Section 5.

4.4 - MILP

The MPEC problem given in Section 4.3 is nonlinear due to the bilinear terms in (19) and the complementarity constraints (33)-(35). To linearize the function (19), the Strong duality theorem is applied to transform it into its equivalent linear function (37) as detailed in Appendix B. On the other hand, the complementarity constraints are linearized using the big-M method [33]. After applying these linearization tricks, the MPEC model given in Section 4.3 can be replaced by the following MILP.

$$\max_{\substack{\mathbf{X}_i^{UL} \cup \mathbf{X}_{primal}^{LL} \cup \\ \alpha_{i,t} \cup \mathbf{X}_{dual}^{LL} \cup \boldsymbol{\Gamma}}} \sum_{\omega\in\Omega} \left\{ \frac{\Delta t}{|\Omega|} \cdot \sum_{t\in\mathbb{T}} \left\{ \begin{array}{c} \sum_{\substack{j\in\mathbb{M} \\ j\neq i}} \left\{ \begin{array}{c} \alpha_{j,t} \cdot \left(p_{i,\omega,t}^{P2P,buy} - p_{i,\omega,t}^{P2P,sell}\right) - \\ \overline{\mu}_{j,\omega,t}^{P2P,buy} \cdot \overline{p}_{j,\omega,t}^{P2P,buy} - \overline{\mu}_{j,\omega,t}^{P2P,sell} \cdot \overline{p}_{j,\omega,t}^{P2P,sell} \end{array} \right\} - \\ \sum_{i\in\mathbb{M}} \left\{ \begin{array}{c} \sum_{n\in\Psi_i} \left\{\pi \cdot \left(\underline{\gamma}_{\omega,n,t} + \overline{\gamma}_{\omega,n,t}\right)\right\} + \\ \sum_{n\in\Psi_i,(m\in\Psi_n)} \left\{\overline{F}_{[n,m]} \cdot \left(\underline{\zeta}_{\omega,[n,m],t} + \overline{\zeta}_{\omega,[n,m],t}\right)\right\} \end{array} \right\} \end{array} \right\} \right\} \quad (37)$$

Subject to (20), (22)-(36) and

$$0 \le u_{v_1} \perp u_{v_2} \ge 0 \equiv \begin{cases} u_{v_1} \ge 0, u_{v_2} \ge 0 \\ u_{v_1} \le M \cdot \xi_v \\ u_{v_1} \le M \cdot (1-\xi_v) \\ \xi_v \in \{0,1\} \end{cases}; \forall v \in \{(31)-(33)\} \quad (38)$$

where $\mathbf{X}_{dual}^{LL}$ is the vector of the lower level dual variables while $\boldsymbol{\Gamma}$ encompasses the auxiliary binary variables ξ's. Note that there are still nonlinearities in the MG operational model (3)-(18). In this case, the quadratic function (4) can be linearized using its piecewise approximation, as described in [34], while the method (38) is also valid to linearize the complementarity constraints (16) and (17).

5 - Solution algorithm based on diagonalization

In competitive MGCs, preserving the privacy of users may be crucial. It is reasonable to think that the different agents partaking in the cluster would be reluctant to share some information with others. In this regard, we develop in this section a privacy-aware EPEC solution methodology.

There exists different algorithms and methodologies that account for privacy issues, some of them were already reviewed in Section 1.2. Most of developed methodologies recur to distributed algorithms, in which each agent is responsible of running some calculations of the optimization procedure. Typically, these calculations only involve data referred to the agent itself, whereas data from others is neglected or directly estimated. Within this kind of algorithms, the alternating direction of multipliers is very popular [13, 15, 21]. However, this methodology might entail computationally issues as it involves some nonlinear terms that require the use of specific solvers. To solve such issue, we developed a fully MILP methodology based on diagonalization, in which only maximum exportable/importable power and bidding/offering prices are shared with the cluster. Note that sharing this kind of data is not problematic normally, as it corresponds with typical information shared in competitive energy markets.

5.1 - EPEC

EPEC-based frameworks are very popular for seeking equilibrium operating conditions among competitive agents [35]. Basically, an EPEC framework consists on solving the equivalent MPEC problem for each agent, concerning for equilibrium constraints among them. For simplicity, Fig. 4 shows a conceptual scheme of EPEC problems involved N agents. Keeping this in mind, an EPEC structure seems suitable for the price setting problem for the MGC described in Section 2. Indeed, in this cluster, different MGs compete with others on a perfect market framework. Thus, the overall optimization model presented in Section 4 is converted to its equivalent EPEC framework, by which the MPEC problem for each MG partaking in the cluster is solved and interact with the other optimal offering strategies, as said (39).

$$\text{solve}\ \text{MPEC}_i\ ; \forall i \in \mathbb{M} \tag{39}$$

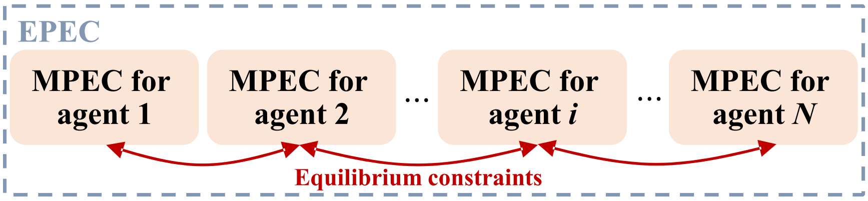

Fig. 4 - Conceptual scheme of an EPEC framework involving N agents

5.2 - Privacy-aware diagonalization algorithm

In general, there exists two approaches for solving EPEC frameworks. On the one hand, each MPEC problem can be transferred by its KKT conditions thus forming a unique optimization framework where the nodal price is set [18]. On the other hand, diagonalization algorithms can be employed, where each MPEC is solved sequentially assuming fixed strategies of the rival players [36]. In this paper, diagonalization has been used due to the following reasons:

- The first approach may result computationally expensive especially if the number of MGs is large and scenarios are considered for uncertainties, which would hinder its applicability in generic stochastic environments.
- The first approach requires perfect knowledge of all the data regarding each MG, which clearly entails privacy issues.

The proposed diagonalization-based algorithm is summarized in the flowchart of Fig. 5 and fully described by the steps 1-6 below, involving two loops whose convergence criteria are given by

$$\left\| \begin{bmatrix} \overline{p}_{i,\omega,t}^{P2P,buy^{(k)}} - \overline{p}_{i,\omega,t}^{P2P,buy^{(k-1)}} \\ \overline{p}_{i,\omega,t}^{P2P,sell^{(k)}} - \overline{p}_{i,\omega,t}^{P2P,sell^{(k-1)}} \end{bmatrix} \Big/ \left[\overline{p}_{i,\omega,t}^{P2P,buy^{(k)}}, \overline{p}_{i,\omega,t}^{P2P,sell^{(k)}} \right] \right\|_{\infty} \leq \epsilon^{MG} \tag{40}$$

$$\left\| \frac{\boldsymbol{\Delta}^{(l)} - \boldsymbol{\Delta}^{(l-1)}}{\boldsymbol{\Delta}^{(l)}} \right\|_{\infty} \leq \epsilon^{EPEC} \tag{41}$$

where $\boldsymbol{\Delta}$ encompasses the offering/bidding prices of all the MGs within the cluster.

1. Initialize the outer iteration counter $k = 1$ and establish tolerances $\epsilon^{MG} \in \mathbb{R}_+$ and $\epsilon^{EPEC} \in \mathbb{R}_+$.
2. Each MG operator solves her operational model (3)-(18). As result, each operator communicates her buyer/seller role together with the maximum importable/exportable power to the coordinator.

3. Sort the MGs (see Section 5.3) and initialize the inner loop iteration counter $l = 1$.
4. The cluster coordinator solves the MPEC problem (20), (22)-(38) for each MG in the order established. After running each MPEC problem, the optimal offering strategy of each MG is updated as $\alpha_{i,t} = \lambda_{n\in\Psi_i,\omega,t}$.
5. If $l = 1$, then set $l = l + 1$ and go to step 4. Otherwise, check the convergence criteria of the inner loop (41). If (41) is met, then go to step 6, otherwise, set $l = l + 1$ and go to step 4.
6. If $k = 1$, then set $k = k + 1$ and go to step 2. Otherwise, check the convergence criteria of the outer loop (42). If (42) is met, then stop, otherwise, set $k = k + 1$ and go to step 2.

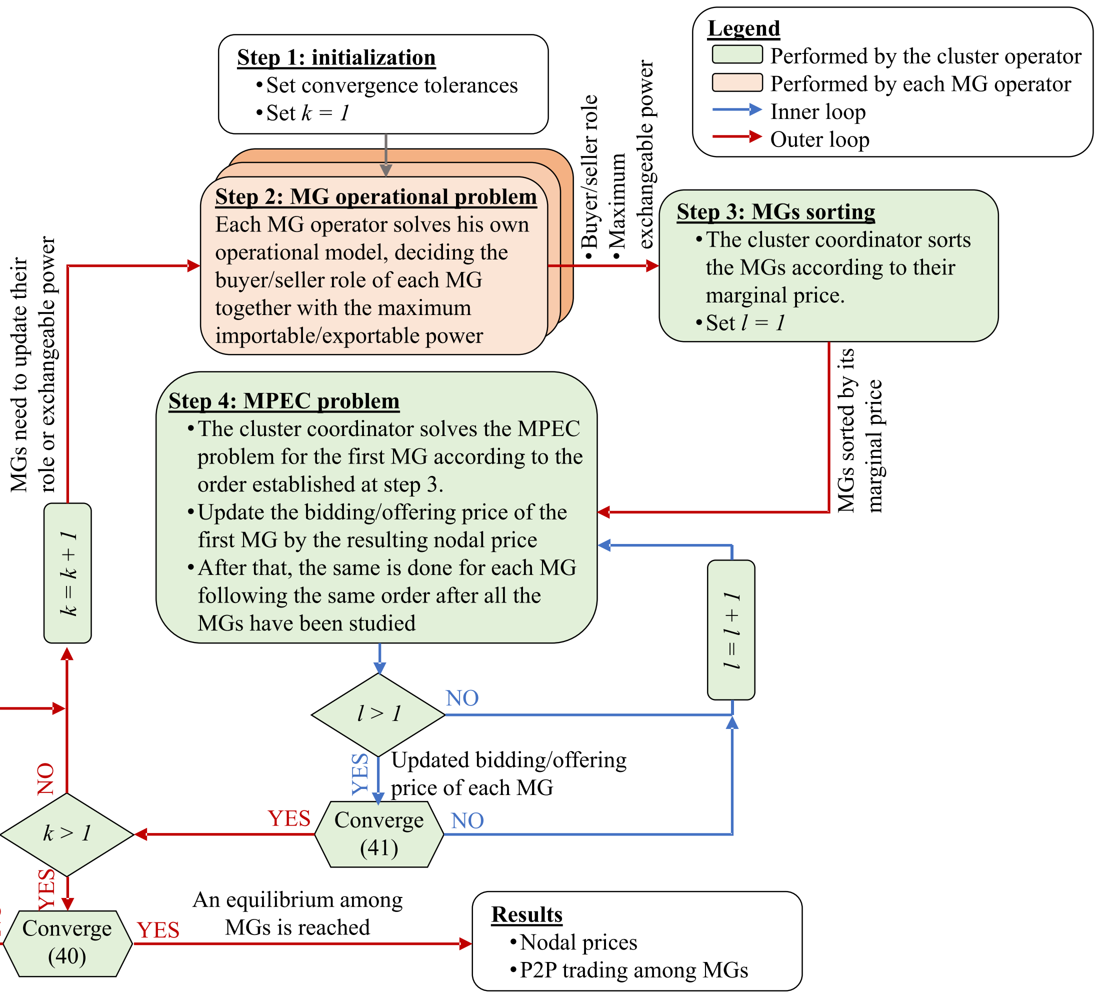

Fig. 5 - Flowchart of the proposed privacy-aware diagonalization algorithm

As seen in Fig. 5, the proposed algorithm preserves the privacy of each user as they only transfer the maximum exportable/importable power together with their bidding/offering price. In addition, this information is not shared with rivals, ensuring that privacy concerns do not discourage MGs to participate in the market mechanism. Furthermore, feasibility of the MG operational model is ensured by updating the bounds in (23) and (24) after running the step 2.

5.3 - Practical considerations

It is important to note that at step 4 of the developed algorithm, the bidding/offering price of each MG equals to the nodal price. However, while the nodal price spans over Ω, the bidding/offering price is not defined for each scenario. To solve this issue, we assume that MG risk strategy is previously agreed with the coordinator, in the sense that the considered nodal price would depend on the risk position of the MG (neutral, averse or seeker). Thus, if a MG adopts a risk-seeker strategy, ω at step 4 corresponds with the best-scenario for uncertainties, taking equivalent decisions for risk-neutral and risk-averse peers. Note that within this framework, each MG can individually adopt its own strategy while previously agreed with the coordinator.

Diagonalization algorithms present two issues that should be considered for successful application of the algorithm developed above. On the one hand, the order in which the MPEC problems are solved may impact on the final solution. Actually, it is observed that diagonalization tends to favour to the first peer analysed in the algorithm, being possible to result in inefficient market mechanisms [18]. To solve this problem, we propose to firstly analyse that MG with the lowest bidding/offering price. This way, the algorithm ensures to favour to the most economical agent, thus leading the algorithm to the a priori most beneficial solution for all the peers partaking in the cluster. On the other hand, the algorithm occasionally tends to oscillate between two possible solutions for a large number of iterations. When this particular behaviour is detected, the algorithm immediately stops and chooses that solution with the highest collective welfare.

Lastly, the optimal offering/bidding strategy of each MG must be fixed at the beginning of the algorithm. Empirical evidences showed us that taking the marginal price of each MG as initial offering/bidding strategy often gives good results, leading to convergence in few iterations.

6 - Case study

This section presents a case study with twofold purpose:

- Validate the developed price-setting model.
- Analyse different relevant aspects like the performance of the proposed diagonalization algorithm, its computational tractability and the impact of uncertainties.

The developed MILP problem has been coded under Matlab R2021a and solved using Gurobi [37]. The optimization problem was solved over a 24-h time horizon, as usual in day-ahead energy markets, taking 1-h for time resolution. Moreover, it is assumed that MGs agree a risk-averse strategy with the coordinator when equalling their bidding/offering strategies to the nodal prices (step 4 of the developed algorithm), at least other is specified.

6.1 - Illustrative 9-bus 4-MGs case

6.1.1 - Input data

For illustrative purposes, the 9-bus 4-MGs cluster depicted in Fig. 5 is studied. The MGs are directly connected to a 9-bus network [38], whose relevant data are collected in Table 2. Data regarding DGs and storage systems are collected in Tables 3 and 4, respectively, while Fig. 6

shows the expected renewable generation together with the non-flexible and flexible demands in each MG (the minimum dispatchable flexible demand is fixed at 80 % of its expected value).

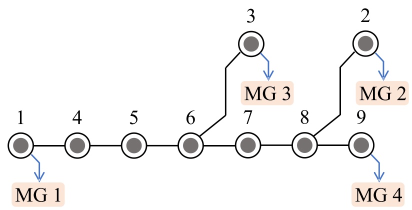

Fig. 5 - The 9-bus 4-MGs system considered in simulations

Table 2 - Network data

Branch	**Res. [Ω]**	**Induct. [Ω]**	**Susc. [Ω^{-1}]**	**Capacity [kVA]**
1-4	0	0.58	0	20,000
4-5	0.17	0.92	0.16	15,000
5-6	0.39	0.17	0.36	15,000
6-3	0	0.6	0	7,000
6-7	0.12	0.1	0.21	9,000
7-8	0.85	0.72	0.15	9,000
8-2	0	0.63	0	7,000
8-9	0.32	0.16	0.31	5,000

Table 3 - Data of DGs

MG	$\overline{p}^{DG}$ **[kW]**	$\underline{p}^{DG}$ **[kW]**	a^{DG} **[$/h]**	b^{DG} **[$/kWh]**	c^{DG} **[$/kWh²]**	RD^{DG}/ RU^{DG} **[kW]**
1	12,000	$0.1 \cdot \overline{p}^{DG}$	0.6	0.05	0.03	$0.5 \cdot \overline{p}^{DG}$
2	10,000	$0.1 \cdot \overline{p}^{DG}$	0.6	0.04	0.02	$0.5 \cdot \overline{p}^{DG}$
3	12,000	$0.1 \cdot \overline{p}^{DG}$	0.6	0.04	0.02	$0.5 \cdot \overline{p}^{DG}$
4	12,000	$0.1 \cdot \overline{p}^{DG}$	0.6	0.07	0.03	$0.5 \cdot \overline{p}^{DG}$

Table 4 - Data of storage systems

MG	$\overline{\varepsilon}^{BES}$ **[kWh]**	$\overline{p}^{BES}$ **[kW]**	$\underline{\varepsilon}^{BES}$ **[kWh]**	η^{BES} **[%]**
1	10,000	$0.2 \cdot \overline{\varepsilon}^{BES}$	$0.25 \cdot \overline{\varepsilon}^{BES}$	95
2	5,000	$0.2 \cdot \overline{\varepsilon}^{BES}$	$0.25 \cdot \overline{\varepsilon}^{BES}$	95
3	5,000	$0.2 \cdot \overline{\varepsilon}^{BES}$	$0.25 \cdot \overline{\varepsilon}^{BES}$	95
4	3,000	$0.2 \cdot \overline{\varepsilon}^{BES}$	$0.25 \cdot \overline{\varepsilon}^{BES}$	95

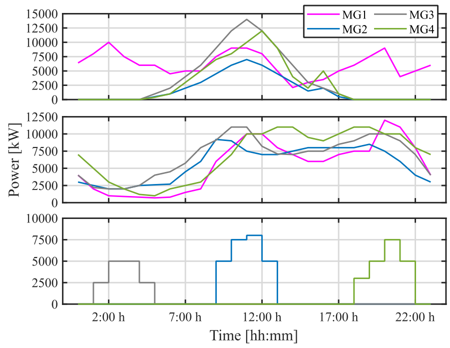

Fig. 6 - Expected renewable generation (top), non-flexible (middle) and flexible (bottom) demand

6.1.2 - Checking the robustness of the uncertainty model

Firstly, let us check the robustness of the proposed interval-based uncertainty modelling described in Section 2. This model aims at capturing extreme realizations for uncertainties, so that the results obtained can be risk-averse, risk-seeker or risk-neutral assuming that uncertainties take their most pessimistic, optimistic or expected values, respectively. To check that this uncertainty model is actually robust, we compare the maximum exportable and importable energy obtained with our approach and the traditional stochastic approach. In this sense, we generate a set of random scenarios within the interval $[\mathrm{E}(\varphi)\cdot 0.75, \mathrm{E}(\varphi)\cdot 1.25]$, which is equivalent to take $CI = 0.25$. Then, the results obtained are compared with the interval notation for the same confidence interval in Fig. 7. As seen in this figure, the results obtained with the considered interval notation always corresponded with more extreme realizations of uncertainties. Indeed, the exportable energy was notably higher for the risk-seeker scenario, which denotes that more renewable potential is assumed to be available in the cluster. In contrast, the exportable energy was lower in case of assuming risk-averse conditions for the same reasons. It is also worth noting that the opposite behaviour is observed for the importable energy, as expected. On the other hand, similar results were obtained in the stochastic and risk-neutral cases, which remarks that stochastic methodologies are actually probabilistic rather than robust. Thus, with the results in Fig. 7 it is clear that the considered interval approach is able to reproduce robust results by only considering extreme values of uncertainties, thus discarding that other intermediate scenarios could yield worse results.

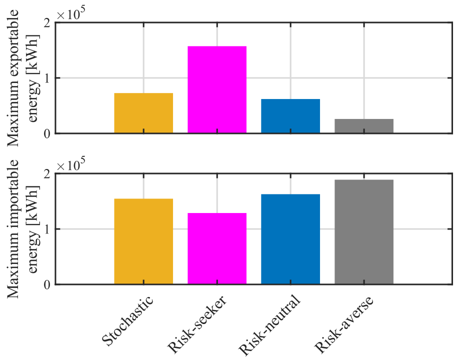

Fig. 7 - Comparison of the maximum exportable (top) and importable (bottom) energy obtained with the considered interval notation and traditional stochastic approach

6.1.3 - Impact of uncertainties

Now, the impact of uncertainties is analysed. Although the optimization framework presented throughout this paper relies on scenario-based foundations, we present the results for the three different scenarios considered namely risk-seeker (favourable realization of uncertainties), risk-neutral (expected profiles) and risk-averse (unfavourable realization of uncertainties). Thereby, Fig. 8 plots the maximum exportable/importable energy of all MGs for various values of the confidence interval. As observed, the maximum exportable energy grew with the interval in the risk-seeker scenario (+57 %), while the importable energy remained almost constant disregarding the value of the confidence interval. In contrast, the exportable energy decreased in the risk-neutral (-7 %) and risk-averse (-61 %) scenarios, observing different trends for the importable energy. This is due to the actual realization considered for uncertainties, since in the risk-seeker scenario the renewable generation increases and the demand is reduced, the exportable energy will increase consequently, while the opposite behaviour is observed in the risk-averse scenario due to the realization of uncertainties. Similar conclusions can be extracted when analysing the total energy exchanged among MGs, which is plotted in Fig. 9. As seen in this figure, the impact of uncertainties varies with the scenario. In this way, while the total energy exchanged increases with the confidence interval in the risk-seeker scenario (+40 %) it decreased in the risk-averse situation (-89 %).

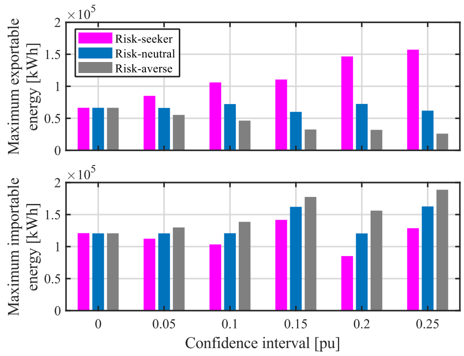

Fig. 8 - Maximum exportable (top) importable (bottom) energy for various scenarios and values of the confidence interval

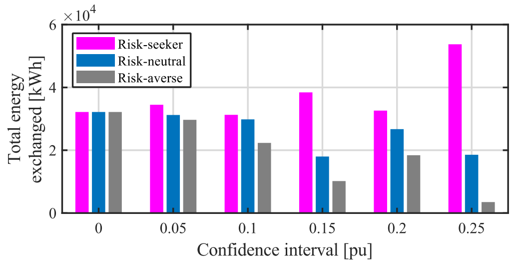

Fig. 9 - Total energy exchanged among MGs for various values of the confidence interval

Fig. 10 plots the energy exchanges among MGs with $CI = 0.05$ and $CI = 0.25$. With $CI = 0.05$, MG1 exports energy to MG2 during night, due to the high renewable penetration in MG1 during this period. During midday, MG3 and MG4 normally became seller and replaced MG1 exporting energy to MG2. This is due to MG3 and MG4 install PV generation, which notably increases during morning and reach its peak production at 12:00 h. It can be clearly observed that energy exchanged was notably lower in the risk-averse scenario when compared with the risk-seeker situation, especially during afternoon due to the pessimistic realization of renewable generation in MG3 and MG4. However, MG1 still exported much energy to MG2 during night. This is due to, despite the negative impact of uncertainties, surplus generation was still high due to the low night demand. In addition, non-flexible demand of MG2 increased in the risk-seeker scenario, leading that more energy is demanded from this MG. On the other hand, when $CI = 0.25$, most of the transactions occurred during midday in the risk-seeker scenario, while energy exchanged was almost null in the risk-averse consideration.

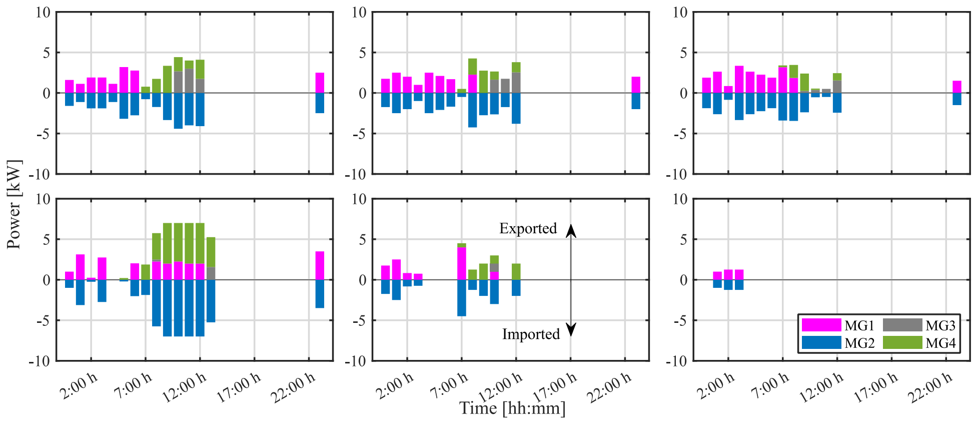

Fig. 10 - Power transactions among MGs with $CI = 0.05$ (top) and $CI = 0.25$ (bottom) in the risk-seeker (left), risk-neutral (middle) and risk-averse (right) scenarios

Now, let us analyse how the uncertainties impact on the nodal prices in Fig. 11. As observed, the average nodal price increased with the confidence interval, only observing marginal variations between scenarios when $CI = 0.25$. This is principally due to bottlenecks in network, which hindered the possibility of exchanging energy among buses throughout the network. This is more clearly observed in Fig. 12, where the average nodal price for each hour of the day is plotted in different situations. As seen, prices were normally equal throughout the network when the confidence interval is low. This is due to, when the influence of uncertainties is marginal, branches are not congested and any bus throughout the grid can trade energy with any other. In contrast, nodal prices varied throughout the network as the confidence interval increases. In fact, nodal prices were normally higher in the risk-seeker scenario and especially during afternoon. This is due to, despite high renewable generation observed during these hours, most of the energy cannot be exported due to branch congestion, thus limiting the actual exportable capacity of some MGs.

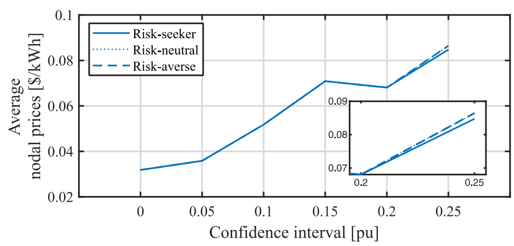

Fig. 11 - Average nodal prices for different values of the confidence interval

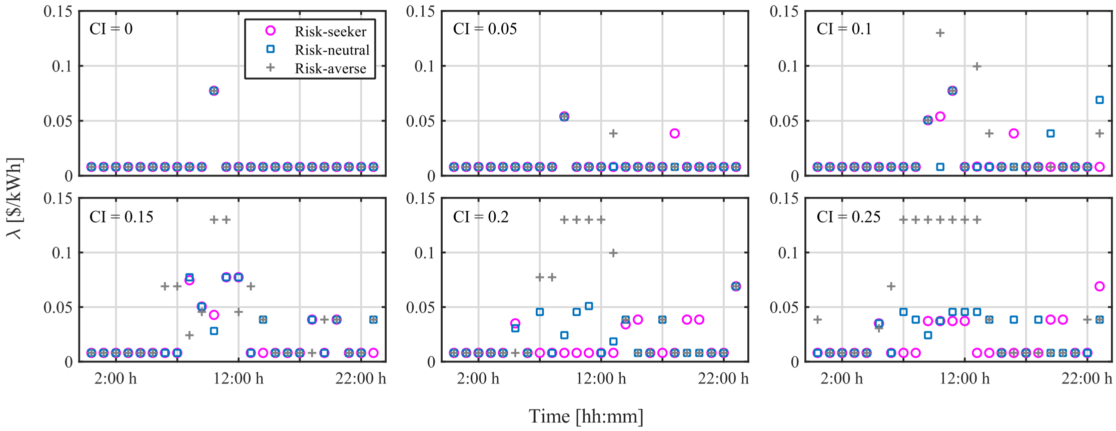

Fig. 12 - Hourly average nodal prices for different scenarios and values of the confidence interval

6.1.4 - Algorithm analysis

Now, the algorithm described in Section 5 is analysed. Fig. 13 plots the evolution of offering/bidding prices of each MG. As observed, when the impact of uncertainties is marginal (low values of the confidence intervals) all the offering/bidding prices evolved to be equal, as already pointed out in Fig. 13. However, the heterogeneity of prices as the confidence interval grows, denoting that some branches throughout the network may experience congestion, leading to price splitting.

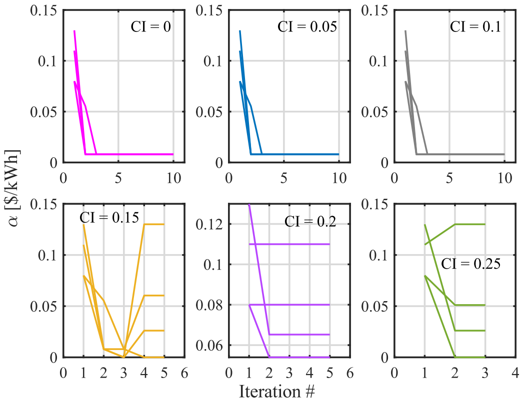

Fig. 13 - Evolution of offering/bidding prices of each MG for various values of the confidence interval

Fig. 14 shows the evolution of the maximum exportable energy of MG1. As observed, when the confidence interval is low and therefore the impact of uncertainties is not critical, this parameter tended to increase as the algorithm evolved, which demonstrates that our proposal is able to foster the participation of peers in energy trading. In contrast, when the confidence interval is higher, the opposite trend was observed since the impact of uncertainties is more notably and pessimistic profiles affect to the risk-neutral and risk-averse scenarios. In Fig. 12 it is clearly observed the oscillatory pattern that occasionally presented the developed algorithm, for which a simple remedy strategy was proposed in Section 5.3.

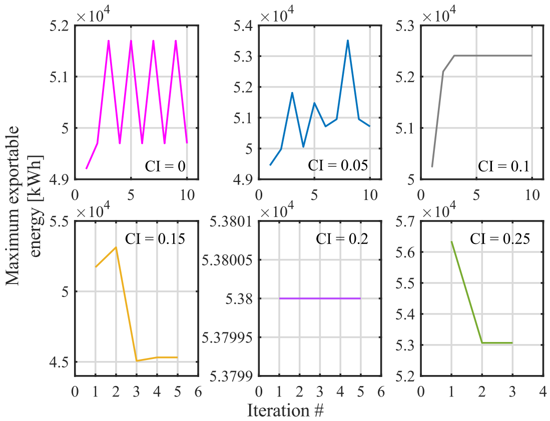

Fig. 14 - Evolution of the maximum exportable energy in MG1

6.2 - Further validation on the IEEE 33-bus system

Next, we further validate the developed tool on a larger system. In this case, we consider the well-known IEEE 33-bus case, whose network parameters can be found in [38]. To keep the model comparable to the previously analysed 9-bus case, we consider 15-MGs in total, connected to the 33-bus network as depicted in Fig. 15. For simplicity, we took the same data for MGs reported in Tables 2-4.

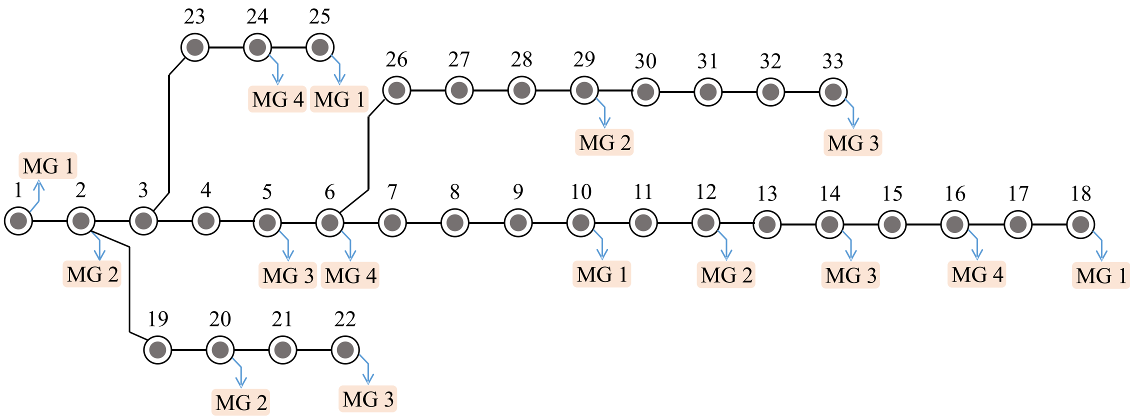

Fig. 15 - The modified IEEE 33-bus case with 15 MGs

In Fig. 16, we compare the maximum exportable energy in the 9-, and 33-bus cases. As expected, the exportable energy was much higher in the 33-bus case, due to the presence of more MGs partaking in the cluster. In fact, the exportable energy was a 25 % higher in the 33-bus case, approximately keeping the proportionality ratio between the two cases (4 MGs vs 15 MGs). In Fig. 16 it is also observed that the confidence interval had a similar impact on this network, decreasing the exportable energy in the risk-averse case when comparing with the risk-neutral and risk-seeker strategies. The number of MGs and number of branches impact directly on the resulting nodal price, as seen in Fig. 17. Indeed, the average nodal pricing was higher in the 33-bus case. This is due to branch congestion is more frequent as the size of the network increases, leading to more isolated sub-systems within the clusters with higher nodal prices.

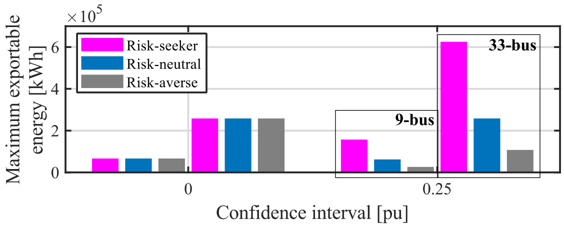

Fig. 16 - Comparison of the maximum exportable energy in the 9-, and 33-bus cases

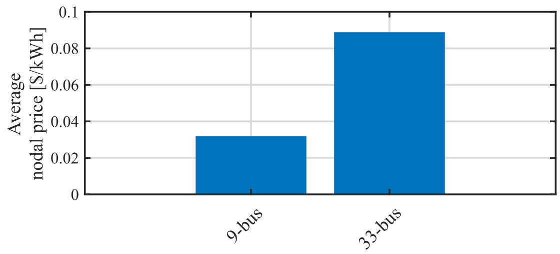

Fig. 17 - Comparison of the average nodal price in the 9-, and 33-bus cases

6.3 - Assessing computational burden

In order to demonstrate the practicability of the developed algorithm, we analyse its computational burden in Table 5. This analysis is presented differentiating relevant procedures within the algorithm. As seen, the outer loop is the costliest part of the developed algorithm. This is due to this step requires to solve the MG operational model each iteration. From our experience, this loop may require a large number of iterations, especially due to oscillatory patterns. Nevertheless, this issue can be partially remedied using the strategy proposed in Section 5.3. On the other hand, the solution of the MG operational model and the inner loop have very few impact on the overall computational performance. In total, the execution of the algorithm does not usually take more than 15 minutes to be executed in the 4-MGs cluster studied in this section. As expected, the total computational time exponentially increased in the 33-bus case. This increment is not only due to the network size and larger number of MGs involved, but also to the increasing number of iterations typically required to reach convergence, which is in concordance with other iterative procedures devoted on analysing medium-, and large-scale networks [39]. In total, the algorithm took approximately 1.5 hours by average, resulting acceptable for a day-ahead tool. Moreover, it should be noted that some parts of the developed algorithm are highly parallelizable, as e.g. the MG operational model, which can be solved for each MG operator in parallel.

Table 5 - Computational performance of the developed algorithm

Part of the algorithm	**Average time [s]**		**Average no. of iterations**	
	9-bus	**33-bus**	**9-bus**	**33-bus**
MG operational model	55	55	--	--
Iteration of the outer loop	78	460	7	8
Iteration of the inner loop	73	400	2	3

7 - Conclusion

A nodal pricing mechanism for islanded MGCs has been presented. The optimization problem is raised as a bi-level model which is transformed into a single-level MPEC using the KKT conditions of the lower level and further linearized using different linearization tricks. The new proposal concerns about privacy issues, for which an original diagonalization algorithm has been developed in which only boundary information is transferred from MGs to the coordinator. Uncertainties from renewable generation and non-flexible demand have been accommodated using interval notation and equivalent scenarios, which results in a light computational framework solvable by off-the-shelf solvers.

A case study was performed on a benchmark 4-MG cluster integrated in a 9-bus network. The results served to analyse the impact of uncertainties in the final results, especially in the total energy exchanged among MGs, which may be reduced with the value of the confidence interval by 61% in the risk-averse scenario. The performance of the developed algorithm has been also analysed, showing that the new proposal encourages the participation of MGs in energy trading, at least when the impact of uncertainties is not notable. These illustrative results were confirmed on a larger network involved 15 MGs. In addition, it was show that computational burden of the proposed methodology is not critical and does not suppose a barrier for the practical application of the developed procedure.

Future works should be focused on extending the ideas drawn in this paper to other related problems where privacy concerns suppose a critical aspect.

Appendix A - Lagrangian function of (19)

The Lagrangian function of (19) is given in (A1), from which the stationary constraints (29)-(32) can be easily derived by taking the first partial derivatives of (A1) w.r.t. $\mathbf{X}_{primal}^{LL}$.

$$\mathcal{L}\left(\mathbf{X}_{primal}^{LL},\mathbf{X}_{dual}^{LL}\right)=\sum_{\omega\in\Omega}\sum_{t\in\mathbb{T}}\left\{\begin{array}{c}\sum_{i\in\mathbb{M}}\left\{\begin{array}{c}\alpha_{i,t}\cdot\left(p_{i,\omega,t}^{P2P,sell}-p_{i,\omega,t}^{P2P,buy}\right)-\\ \underline{\mu}_{i,\omega,t}^{P2P,buy}\cdot p_{i,\omega,t}^{P2P,buy}-\underline{\mu}_{i,\omega,t}^{P2P,sell}\cdot p_{i,\omega,t}^{P2P,sell}\\ +\overline{\mu}_{i,\omega,t}^{P2P,buy}\cdot\left(p_{i,\omega,t}^{P2P,buy}-\overline{p}_{i,\omega,t}^{P2P,buy}\right)\\ +\overline{\mu}_{i,\omega,t}^{P2P,sell}\cdot\left(p_{i,\omega,t}^{P2P,sell}-\overline{p}_{i,\omega,t}^{P2P,sell}\right)\end{array}\right\}+\\ \sum_{n,m\in\Psi}\left\{\begin{array}{c}\overline{\zeta}_{\omega,[n,m],t}\cdot\left(F_{\omega,[n,m],t}-\overline{F}_{[n,m]}\right)\\ -\underline{\zeta}_{\omega,[n,m],t}\cdot\left(F_{\omega,[n,m],t}+\overline{F}_{[n,m]}\right)\end{array}\right\}+\\ \sum_{n\in\Psi}\left\{\begin{array}{c}\overline{\gamma}_{\omega,n,t}\cdot\left(\theta_{\omega,n,t}-\pi\right)-\\ \underline{\gamma}_{\omega,n,t}\cdot\left(\theta_{\omega,n,t}+\pi\right)\end{array}\right\}+\gamma_{\omega,ref,t}\cdot\theta_{\omega,ref,t}+\\ \sum_{n,(m\in\Psi_n)}\lambda_{n,\omega,t}\cdot\left\{\begin{array}{c}\sum_{m\in\Psi_n}B_{[n,m]}\cdot\left(\theta_{\omega,n,t}-\theta_{\omega,m,t}\right)\\ +\sum_{i\in\Psi_n}\left(p_{i,\omega,t}^{P2P,buy}-p_{i,\omega,t}^{P2P,sell}\right)\end{array}\right\}\end{array}\right\} \quad \text{(A1)}$$

Appendix B - Linearization of (19)

Subsequent steps detail the process of linearizing the bi-linear term $\lambda_{n\in\Psi_{i},\omega,t}\cdot\left(p_{i,\omega,t}^{P2P,sell}-p_{i,\omega,t}^{P2P,buy}\right)$ appeared in (19) to finally result in the linear function (37). Applying Strong duality theorem to (19) yields

$$\sum_{\omega\in\Omega}\sum_{i\in\mathbb{M}}\sum_{t\in\mathbb{T}}\left\{\alpha_{i,t}\cdot\left(p_{i,\omega,t}^{P2P,sell}-p_{i,\omega,t}^{P2P,buy}\right)\right\}=$$

$$\sum_{\omega\in\Omega}\sum_{i\in\mathbb{M}}\sum_{t\in\mathbb{T}}\left\{\begin{array}{c}-\overline{\mu}_{i,\omega,t}^{P2P,buy}\cdot\overline{p}_{i,\omega,t}^{P2P,buy}-\overline{\mu}_{i,\omega,t}^{P2P,sell}\cdot\overline{p}_{i,\omega,t}^{P2P,sell}\\ -\sum_{n\in\Psi_i}\left\{\pi\cdot\left(\underline{\gamma}_{\omega,n,t}+\overline{\gamma}_{\omega,n,t}\right)\right\}\\ -\sum_{n\in\Psi_i,(m\in\Psi_n)}\left\{\overline{F}_{[n,m]}\cdot\left(\underline{\zeta}_{\omega,[n,m],t}+\overline{\zeta}_{\omega,[n,m],t}\right)\right\}\end{array}\right\} \qquad \text{(B1)}$$

From (29) and (30) one has

$$\left\{\begin{array}{c}\alpha_{i,t}\cdot p_{i,\omega,t}^{P2P,sell}-\underline{\mu}_{i,\omega,t}^{P2P,sell}\cdot p_{i,\omega,t}^{P2P,sell}+\\ \overline{\mu}_{i,\omega,t}^{P2P,sell}\cdot p_{i,\omega,t}^{P2P,sell}-\lambda_{n\in\Psi_i,\omega,t}\cdot p_{i,\omega,t}^{P2P,sell}=0\end{array}\right.;\forall i\in\mathbb{M}\wedge\omega\in\Omega\wedge t\in\mathbb{T} \qquad \text{(B2)}$$

$$\left\{\begin{array}{c}-\alpha_{i,t}\cdot p_{i,\omega,t}^{P2P,buy}-\underline{\mu}_{i,\omega,t}^{P2P,buy}\cdot p_{i,\omega,t}^{P2P,buy}+\\ \overline{\mu}_{i,\omega,t}^{P2P,buy}\cdot p_{i,\omega,t}^{P2P,buy}+\lambda_{n\in\Psi_i,\omega,t}\cdot p_{i,\omega,t}^{P2P,buy}=0\end{array}\right.;\forall i\in\mathbb{M}\wedge\omega\in\Omega\wedge t\in\mathbb{T} \qquad \text{(B3)}$$

From complementarity condition (33), the following equality holds

$$\left\{\begin{array}{c}\overline{\mu}_{i,\omega,t}^{P2P,x}\cdot p_{i,\omega,t}^{P2P,x}=\overline{\mu}_{i,\omega,t}^{P2P}\cdot\overline{p}_{i,\omega,t}^{P2P,x}\\ \underline{\mu}_{i,\omega,t}^{P2P,x}\cdot p_{i,\omega,t}^{P2P,x}=0\end{array}\right.;\forall i\in\mathbb{M}\wedge\omega\in\Omega\wedge t\in\mathbb{T}\wedge x\in\{buy,sell\} \qquad \text{(B4)}$$

Replacing (B4) into (B2) and (B3) yields

$$\left\{\begin{array}{c}\alpha_{i,t}\cdot p_{i,\omega,t}^{P2P,sell}+\\ \overline{\mu}_{i,\omega,t}^{P2P,sell}\cdot\overline{p}_{i,\omega,t}^{P2P,sell}-\\ \lambda_{n\in\Psi_i,\omega,t}\cdot p_{i,\omega,t}^{P2P,sell}=0\end{array}\right.;\forall i\in\mathbb{M}\wedge\omega\in\Omega\wedge t\in\mathbb{T} \qquad \text{(B5)}$$

$$\left\{\begin{array}{c}-\alpha_{i,t}\cdot p_{i,\omega,t}^{P2P,buy}+\\ \overline{\mu}_{i,\omega,t}^{P2P,buy}\cdot\overline{p}_{i,\omega,t}^{P2P,buy}+\\ \lambda_{n\in\Psi_i,\omega,t}\cdot p_{i,\omega,t}^{P2P,buy}=0\end{array}\right.;\forall i\in\mathbb{M}\wedge\omega\in\Omega\wedge t\in\mathbb{T} \qquad \text{(B6)}$$

Rearranging (B5) and (B6) one obtains

$$\alpha_{i,t}\cdot p_{i,\omega,t}^{P2P,sell}=\lambda_{n\in\Psi_i,\omega,t}\cdot p_{i,\omega,t}^{P2P,sell}-\overline{\mu}_{i,\omega,t}^{P2P,sell}\cdot\overline{p}_{i,\omega,t}^{P2P,sell};\forall i\in\mathbb{M}\wedge\omega\in\Omega\wedge t\in\mathbb{T} \qquad \text{(B7)}$$

$$-\alpha_{i,t}\cdot p_{i,\omega,t}^{P2P,buy}=-\lambda_{n\in\Psi_i,\omega,t}\cdot p_{i,\omega,t}^{P2P,buy}-\overline{\mu}_{i,\omega,t}^{P2P,buy}\cdot\overline{p}_{i,\omega,t}^{P2P,buy};\forall i\in\mathbb{M}\wedge\omega\in\Omega\wedge t\in\mathbb{T} \qquad \text{(B8)}$$

Replacing (B7) and (B8) into (B1) yields

$$\sum_{\omega\in\Omega}\sum_{t\in\mathbb{T}}\left\{\begin{array}{c}\lambda_{n\in\Psi_i,\omega,t}\cdot\left(p_{i,\omega,t}^{P2P,sell}-p_{i,\omega,t}^{P2P,buy}\right)\\ -\overline{\mu}_{i,\omega,t}^{P2P,buy}\cdot\overline{p}_{i,\omega,t}^{P2P,buy}-\overline{\mu}_{i,\omega,t}^{P2P,buy}\cdot\overline{p}_{i,\omega,t}^{P2P,buy}\\ +\sum_{\substack{j\in\mathbb{M}\\ j\neq i}}\left\{\alpha_{j,t}\cdot\left(p_{i,\omega,t}^{P2P,sell}-p_{i,\omega,t}^{P2P,buy}\right)\right\}\end{array}\right\}=$$

$$\sum_{i\in\mathbb{M}}\sum_{\omega\in\Omega}\sum_{t\in\mathbb{T}}\left\{\begin{array}{c}-\overline{\mu}_{i,\omega,t}^{P2P,buy}\cdot\overline{p}_{i,\omega,t}^{P2P,buy}-\overline{\mu}_{i,\omega,t}^{P2P,sell}\cdot\overline{p}_{i,\omega,t}^{P2P,sell}\\ -\sum_{n\in\Psi_i}\left\{\pi\cdot\left(\underline{\gamma}_{\omega,n,t}+\overline{\gamma}_{\omega,n,t}\right)\right\}\\ -\sum_{n\in\Psi_i,(m\in\Psi_n)}\left\{\overline{F}_{[n,m]}\cdot\left(\underline{\zeta}_{\omega,[n,m],t}+\overline{\zeta}_{\omega,[n,m],t}\right)\right\}\end{array}\right\} \qquad \text{(B9)}$$

Rearranging (B9) one finally has

$$\sum_{\omega\in\Omega}\left\{\frac{\Delta t}{|\Omega|}\cdot\sum_{t\in\mathbb{T}}\left\{\lambda_{n\in\Psi_i,\omega,t}\cdot\left(p_{j,\omega,t}^{P2P,buy}-p_{i,\omega,t}^{P2P,sell}\right)\right\}\right\}=\sum_{\omega\in\Omega}\left\{\frac{\Delta t}{|\Omega|}\cdot\right.$$

$$\left.\sum_{t\in\mathbb{T}}\left\{\begin{array}{c}\sum_{\substack{j\in\mathbb{M}\\ j\neq i}}\left\{\begin{array}{c}\alpha_{j,t}\cdot\left(p_{i,\omega,t}^{P2P,sell}-p_{i,\omega,t}^{P2P,buy}\right)+\\ \overline{\mu}_{j,\omega,t}^{P2P,buy}\cdot\overline{p}_{j,\omega,t}^{P2P,buy}+\overline{\mu}_{j,\omega,t}^{P2P,sell}\cdot\overline{p}_{j,\omega,t}^{P2P,sell}\end{array}\right\}+\\ \sum_{i\in\mathbb{M}}\left\{\begin{array}{c}\sum_{n\in\Psi_i}\left\{\pi\cdot\left(\underline{\gamma}_{\omega,n,t}+\overline{\gamma}_{\omega,n,t}\right)\right\}+\\ \sum_{n\in\Psi_i,(m\in\Psi_n)}\left\{\overline{F}_{[n,m]}\cdot\left(\underline{\zeta}_{\omega,[n,m],t}+\overline{\zeta}_{\omega,[n,m],t}\right)\right\}\end{array}\right\}\end{array}\right\}\right\} \quad \text{(B10)}$$

Acknowledgments

The authors wish to thank to the Spanish Ministry of Science and Innovation, under the research Project "Desarrollo de modelos de flujos de carga para clusters de microrredes" (PID2021-123633OB).

References

[1] D. Neves, A. Pina, C.A. Silva. Demand response modeling: A comparison between tools. *Applied Energy* 2015; 146: 288-97. https://doi.org/10.1016/j.apenergy.2015.02.057.

[2] M. Tostado-Véliz, S. Kamel, F. Aymen, A.R. Jordehi, F. Jurado. A Stochastic-IGDT model for energy management in isolated microgrids considering failures and demand response. *Applied Energy* 2022; 317: 119162. https://doi.org/10.1016/j.apenergy.2022.119162.

[3] S. Tan, P. Xie, J.M. Guerrero, J.C. Vasquez. False Data Injection Cyber-Attacks Detection for Multiple DC Microgrid Clusters. *Applied Energy* 2022; 310: 118425. https://doi.org/10.1016/j.apenergy.2021.118425.

[4] H. Ruan, H. Gao, H.B. Gooi, J. Liu. Active distribution network operation management integrated with P2P trading. *Applied Energy* 2022; 323: 119632. https://doi.org/10.1016/j.apenergy.2022.119632.

[5] H. Lin, C. Liu, J.M. Guerrero, J.C. Vasquez, T. Dragicevic. Modular Power Architectures for Microgrid Clusters. In *2014 International Conference on Green Energy* 2014; Sfax, Tunisia: 199-206. https://doi.org/10.1109/ICGE.2014.6835422.

[6] M. Jalali, K. Zare, H. Seyedi. Strategic decision-making of distribution network operator with multi-microgrids considering demand response program. *Energy* 2017; 141: 1059-71. https://doi.org/10.1016/j.energy.2017.09.145.

[7] Y. Liu, L. Guo, C. Wang. A robust operation-based scheduling optimization for smart distribution networks with multi-microgrids. *Applied Energy* 2018; 228: 130-40. https://doi.org/10.1016/j.apenergy.2018.04.087.

[8] H. Qiu, B. Zhao, W. Gu, R. Bo. Bi-Level Two-Stage Robust Optimal Scheduling for AC/DC Hybrid Multi-Microgrids. *IEEE Transactions on Smart Grid* 2018; 9(5): 5455-66. https://doi.org/10.1109/TSG.2018.2806973.

[9] C. Zhang, J. Wu, Y. Zhou, M. Cheng, C. Long. Peer-to-Peer energy trading in a Microgrid. *Applied Energy* 2018; 220: 1-12. https://doi.org/10.1016/j.apenergy.2018.03.010.

[10] A. N. Toutounchi, S. Seyedshenava, J. Contreras, A. Akbarimajd. A Stochastic Bilevel Model to Manage Active Distribution Networks With Multi-Microgrids. *IEEE Systems Journal* 2019; 13(4): 4190-9. https://doi.org/10.1109/JSYST.2018.2890062.

[11] X. Zhou, Q. Ai. Distributed economic and environmental dispatch in two kinds of CCHP microgrid clusters. *International Journal of Electrical Power & Energy Systems* 2019; 112: 109-26. https://doi.org/10.1016/j.ijepes.2019.04.045.

[12] F. Khavari, A. Badri, A. Zangeneh. Energy management in multi-microgrids via an aggregator to override point of common coupling congestion. *IET Generation, Transmission & Distribution* 2019; 13(5): 634-42. https://doi.org/10.1049/iet-gtd.2018.5922.

[13] S. Lilla, C. Orozco, A. Borghetti, F. Napolitano, F. Tossani. Day-Ahead Scheduling of a Local Energy Community: An Alternating Direction Method of Multipliers Approach. *IEEE*

Transactions on Power Systems 2020; 35(2): 1132-42. https://doi.org/10.1109/TPWRS.2019.2944541.

[14] X. Zhou, Q. Ai, M. Yousif. Two kinds of decentralized robust economic dispatch framework combined distribution network and multi-microgrids. *Applied Energy* 2019; 253: 113588. https://doi.org/10.1016/j.apenergy.2019.113588.

[15] Y. Zhang, Q. Ai, H. Wang, Z. Li, K. Huang. Bi-level distributed day-ahead schedule for islanded multi-microgrids in a carbon trading market. *Electric Power Systems Research* 2020; 186: 106412. https://doi.org/10.1016/j.epsr.2020.106412.

[16] D.L. Rodrigues, X. Ye, X. Xia, B. Zhu. Battery energy storage sizing optimisation for different ownership structures in a peer-to-peer energy sharing community. *Applied Energy* 2020; 262: 114498. https://doi.org/10.1016/j.apenergy.2020.114498.

[17] Y. Fu, Z. Zhang, Z. Li and Y. Mi. Energy Management for Hybrid AC/DC Distribution System With Microgrid Clusters Using Non-Cooperative Game Theory and Robust Optimization. *IEEE Transactions on Smart Grid* 2020; 11(2): 1510-25. https://doi.org/10.1109/TSG.2019.2939586.

[18] A. Naebi, S.S. Shenava, J. Contreras, C. Ruiz, A. Akbarimajd. EPEC approach for finding optimal day-ahead bidding strategy equilibria of multi-microgrids in active distribution networks. *International Journal of Electrical Power & Energy Systems* 2020; 117: 105702. https://doi.org/10.1016/j.ijepes.2019.105702.

[19] Q. Xu, Y. Xu, Z. Xu, L. Xie, F. Blaabjerg. A Hierarchically Coordinated Operation and Control Scheme for DC Microgrid Clusters Under Uncertainty. *IEEE Transactions on Sustainable Energy* 2021; 12(1): 273-83. https://doi.org/10.1109/TSTE.2020.2991096.

[20] H. Nezamabadi, V. Vahidinasab. Arbitrage Strategy of Renewable-Based Microgrids via Peer-to-Peer Energy-Trading. *IEEE Transactions on Sustainable Energy* 2021; 12(2): 1372-82. https://doi.org/10.1109/TSTE.2020.3045216.

[21] J. Guo et al. Decentralized Incentive-based multi-energy trading mechanism for CCHP-based MG cluster. *International Journal of Electrical Power & Energy Systems* 2021; 133: 107138. https://doi.org/10.1016/j.ijepes.2021.107138.

[22] M. Yan, M. Shahidehpour, A. Paaso, L. Zhang, A. Alabdulwahab, A. Abusorrah. Distribution Network-Constrained Optimization of Peer-to-Peer Transactive Energy Trading Among Multi-Microgrids. *IEEE Transactions on Smart Grid* 2021; 12(2): 1033-47. https://doi.org/10.1109/TSG.2020.3032889.

[23] P. Sheikhahmadi, S. Bahramara, A. Mazza, G. Chicco, M. Shafie-Khah, J.P.S. Catalão. Multi-Microgrids Operation With Interruptible Loads in Local Energy and Reserve Markets. *IEEE Systems Journal* 2022; Early access. https://doi.org/10.1109/JSYST.2022.3177637.

[24] N. Vespermann, T. Hamacher, J. Kazempour. Risk Trading in Energy Communities. *IEEE Transactions on Smart Grid* 2021; 12(2): 1249-63. https://doi.org/10.1109/TSG.2020.3030319.

[25] C. Orozco, A. Borghetti, B. De Schutter, F. Napolitano, G. Pulazza, F. Tossani. Intra-day scheduling of a local energy community coordinated with day-ahead multistage decisions. *Sustainable Energy Grids & Networks* 2022; 29: 100573. https://doi.org/10.1016/j.segan.2021.100573.

[26] S. Haghifam, H. Laaksonen, M. Shafie-Khah. Modeling a Local Electricity Market for Transactive Energy Trading of Multi-Aggregators. *IEEE Access* 2022; 10: 68792-806. https://doi.org/10.1109/ACCESS.2022.3186309.

[27] A. Conejo, M. Carrión, J.M. Morales. *Decision Making Under Uncertainty in Electricity Markets*. New York: Springer; 2010.

[28] M. Tostado-Véliz, S. Kamel, H.M. Hasanien, P. Arévalo, R.A. Turky, F. Jurado. A stochastic-interval model for optimal scheduling of PV-assisted multi-mode charging stations. *Energy* 2022; 253: 124219. https://doi.org/10.1016/j.energy.2022.124219.

[29] M. Tostado-Véliz, A.R. Jordehi, S.A. Mansouri, F. Jurado. A two-stage IGDT-stochastic model for optimal scheduling of energy communities with intelligent parking lots. *Energy* 2023; 263(D): 126018. https://doi.org/10.1016/j.energy.2022.126018.

[30] X. Wang et al. Tri-level hybrid interval-stochastic optimal scheduling for flexible residential loads under GAN-assisted multiple uncertainties. *International Journal of Electrical Power & Energy Systems* 2023; 146: 108672. https://doi.org/10.1016/j.ijepes.2022.108672.

[31] M. Tostado-Véliz, S. Kamel, H.M. Hasanien, R.A. Turky, F. Jurado. A mixed-integer-linear-logical programming interval-based model for optimal scheduling of isolated microgrids with green hydrogen-based storage considering demand response. *Journal of Energy Storage* 2022; 48: 104028. https://doi.org/10.1016/j.est.2022.104028.

[32] N. Vespermann, T. Hamacher, J. Kazempour. Risk Trading in Energy Communities. *IEEE Transactions on Smart Grid* 2021; 12(2): 1249-63. https://doi.org/10.1109/TSG.2020.3030319.

[33] X. Wang, F. Li, Q. Zhang, Q. Shi, J. Wang. Profit-Oriented BESS Siting and Sizing in Deregulated Distribution Systems. *IEEE Transactions on Smart Grid*; Early access. https://doi.org/10.1109/TSG.2022.3150768.

[34] S.A. Habeeb, M. Tostado-Véliz, H.M. Hasanien, R.A. Turky, W.K. Meteab, F. Jurado. DC Nanogrids for Integration of Demand Response and Electric Vehicle Charging Infrastructures: Appraisal, Optimal Scheduling and Analysis. *Electronics* 2021; 10(20): 2484. https://doi.org/10.3390/electronics10202484.

[35] S. Gabriel, A. Conejo, J. Fuller, B. Hobbs, C. Ruiz. *Complementarity Modeling in Energy Markets*. New York: Springer; 2012.

[36] S. Wogrin, J. Barquín, E. Centeno. Capacity Expansion Equilibria in Liberalized Electricity Markets: An EPEC Approach. *IEEE Transactions on Power Systems* 2013; 28(2): 1531-9. https://doi.org/10.1109/TPWRS.2012.2217510.

[37] Gurobi Optimization L.L.C. Gurobi Optimizer Reference Manual, 2021. Online, available at: https://www.gurobi.com, accessed Nov. 29, 2022.

[38] R.D. Zimmerman, C.E. Murillo-Sánchez, R.J. Thomas. MATPOWER: Steady-State Operations, Planning, and Analysis Tools for Power Systems Research and Education. *IEEE Transactions on Power Systems* 2011; 26(1): 12-9. https://doi.org/10.1109/TPWRS.2010.2051168.

[39] M. Tostado-Véliz, S. Kamel, F. Jurado. Power Flow Approach Based on the S-Iteration Process. *IEEE Transactions on Power Systems* 2020; 35(6): 4148-58. https://doi.org/10.1109/TPWRS.2020.2989270.